NUMERICAL SIMULATION OF SUPERSONIC FLOW OVER A FLAT PLATE

Shashi Kumar

A Dissertation Submitted to
Indian Institute of Technology Hyderabad
In Partial Fulfillment of the Requirements for
The Degree of Master of Technology

भारतीय प्रौद्योगिकी संस्थान हैदराबाद
Indian Institute of Technology Hyderabad

Department of Mechanical & Aerospace Engineering

June, 2014

Declaration

I declare that this written submission represents my ideas in my own words, and where others' ideas or words have been included, I have adequately cited and referenced the original sources. I also declare that I have adhered to all principles of academic honesty and integrity and have not misrepresented or fabricated or falsified any idea/data/fact/source in my submission. I understand that any violation of the above will be a cause for disciplinary action by the Institute and can also evoke penal action from the sources that have thus not been properly cited, or from whom proper permission has not been taken when needed.

(Signature)

(Shashi Kumar)

(ME12M1024)

Approval Sheet

This thesis entitled 'Numerical Simulation of Supersonic Flow Over a Flat Plate' by Shashi Kumar is approved for the degree of Master of Technology from IIT Hyderabad.

(Dr. Kirti Chandra Sahu) External Examiner
Dept. of Chemical Engg
IITH

(Dr. Pankaj Kolhe) Internal Examiner
Dept. of Mechanical & Aerospace Engg.
IITH

(Dr. K. Venkatasubbaiah) Adviser
Dept. of Mechanical & Aerospace Engg.
IITH

(Dr. Kirti Chandra Sahu) Chairman
Dept. of Chemical Engg
IITH

Acknowledgements

I express my sincere gratitude to my thesis adviser Dr. K. Venkatasubbaiah for his valuable guidance, timely suggestions and constant encouragement. His interest and confidence in me has helped immensely for the successful completion of this work. I would like to thank my classmates Neelapu Satish, Ashwani Asam, Anil B. wakale, for their valuable help and support.

I would like to thank Rahul Patil, Narendra Patel, Neeraj Kumar, Ravi Teja, Vaibhav Garg and all 1000 series friends for making my stay at IIT Hyderabad memorable and enjoyable. Also were always besides me during the happy and hard moments to push me and motivate me.

Last but not the least, I would like to pay high regards to my parents Mr. Ashok Kumar, Mrs. Meena Devi, elder brother Mr Ravi Kumar for their encouragement, inspiration and lifting me uphill this phase of life. I also would like to thank my beloved younger sister Khushboo and younger brother Sunny for their encouragement. I owe everything to them.

Dedicated to

My beloved family

Abstract

Supersonic flow over a flat plate has been investigated numerically. Supersonic flow problem is formulated by a two dimensional compressible unsteady flow with variable properties. The unsteady compressible Navier-Stokes equations are solved by finite difference method. Air is considered as calorically perfect gas, with a constant Prandtl number. The viscosity varies with temperature is modeled by Sutherland's law. The governing equations are solved using a MacCormack time marching technique with central finite difference scheme for spatial discretization. Result are reported for different Mach numbers varies from Ma = 2 to 8. Effects of Mach number on shock boundary layer interactions are reported here. The pressure, velocity and temperature profiles are reported. Result show that the shock strength increases with increase in Mach number. Present results are validated with the results available in the literature.

Nomenclature

ρ	Density
c_p	Pressure coefficient
E_t	Total energy
L	reference length (forward flat plate length in present studies)
M	Mach number
P	pressure
Pr	Prandtl number
q_x	Heat flux in x direction
q_y	Heat flux in y direction
Re	Reynolds number
T	Temperature
u	Velocity in x-direction
v	Velocity in y-direction
e	Internal energy
∞	Free stream conditions
μ	Dynamic viscosity
*	dimension less quantity
t	time

Contents

Chapter 1

Introduction

1.1 Motivation

In recent years aerospace technology development community is showing interest for hypersonic flight vehicles such as long-range passenger transport, reusable launch vehicles for space applications, and long-range missiles. The understanding of shock/boundary layer interactions is import for design of hypersonic scramjet inlets. Study of supersonic flow is an extreme interest today due to its wide application in aerospace engineering, gas dynamics, jet engine, high speed vehicle components, high speed turbo compressor, and missile and rocket propulsions. In literature detailed study of shock/boundary layer interactions are limited. This has been the motivation for present investigation.

1.2 Literature review

Supersonic flow has been an area of research from many decades. Fundamental concepts of supersonic fluid flow are discussed by authors such as Anderson [1], Schichting [5], and Chung [8], who describe different numerical techniques and, most importantly for compressible fluid flow discuss the boundary conditions that should be used at various boundaries. Some notable recent developments for the solution of NS equation based on explicit Runge-Kutta schemes are the work of Jameson et al.[9] and Rizzi and Eriksson.[10].

These books compile the work of the many people who worked to develop different schemes for accurately simulating the supersonic fluid flow. MacCormack (1969) developed the MacCormack scheme [4]. The work of Steger and Warming [25], Roe [26], Van Leer[27], Osher and Chakravarthy [28], and Marten's TVD methods all fall in this category. Although it will not be shown here for every case, these schemes are all equivalent to a central differencing scheme plus some form of dissipation.

Navier Stokes equations suffer from numerical instability, due to lack of the stabilizing viscous terms. This was addressed in early work by adding viscosity artificially to the discretized equations. So the MacCormack scheme with Jameson artificial viscosity was used by many researchers to solve practical problems.

Most of the airborne vehicle in the atmosphere uses the study of aerodynamics over flat surfaces-stationary or moving. In addition we can have ramp or curved surfaces for the study [29].

Gold man et al, have experimentally studied unsteady control surface loads of reentry vehicle at supersonic flight conditions. The observation of the experiment includes instability of a type that involved a fluid dynamical self-excitation of the separated pocket feeding upon or modulated by tunnel. Subsequently, Degani et al [30], had carried out study of Navier stroke solution of an unsteady ramp movement from 15 to 24 degrees. The study was mainly to compare the Navier-stroke solution with thin layer theory and concluded that both the results are comparable. Park et al. [31], had carried out numerical study of inviscid supersonic flow past an unsteady compression ramp. The study revealed that unsteady flow of moving ramp could be considered as steady or quasi study when the non-dimensional angular velocity of the ramp was relatively small. Park et al [32], as continuation to their previous study investigated 2-D viscous supersonic flow at 3 Mach over moving ramp is also helpful in this study.

For the solution of non-linear equations, the more general concept of bounded total variation of solutions was introduced by Harten [33].

1.2 Objective of the present study

Objective of the present study is to understand the shock/boundary layer interactions with different free stream Mach numbers.

1. To develop the compressible Navier-Stokes solver.
2. To study the effect of free stream Mach number on shock/boundary layer interactions
3. To study the effect of viscous on shock patterns.
4. To study the effect of surface temperature on shock /boundary layer interactions

1.4 Thesis organization

Thesis is organized in the following way. Chapter 2 deals with the governing equations, problem definition boundary conditions. Chapter 3 includes the numerical schemes. Chapter 4 deals with results and discussion.

Chapter 2

2.1 Problem Definition

Consider the supersonic flow over a thin sharp flat plate at zero incidence and of length L, as sketched in Fig. 1. A laminar boundary layer develops at the leading edge of the flat plate and remains laminar for the case of relatively low Reynolds number. The oncoming free stream no longer "sees" a sharp flat plate. Rather, due to the presence of the viscous boundary layer, the plate possesses a fictitious curvature. Consequently, a curved induced shock wave, as shown in Fig. 1, is generated at the leading edge. The region between the surface and the shock is called the shock layer. Depending on Mach number, Reynolds number, and surface temperature, the shock layer can be characterized by a region of viscous flow and inviscid flow (refer to Fig.2a), or the entire layer can be fully viscous, a so-called' merged shock layer (Fig.2b). Furthermore, dissipation of kinetic energy within the boundary layer (viscous dissipation) can cause high flow-field temperatures and thus high heat-transfer rates. We are considered the simple geometry to understand the physics of shock/boundary layer interactions.

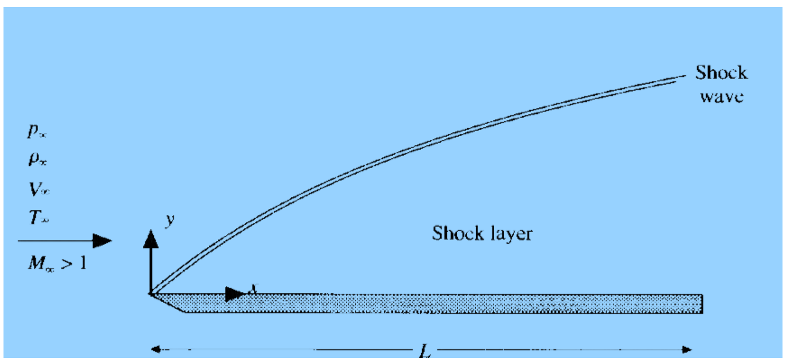

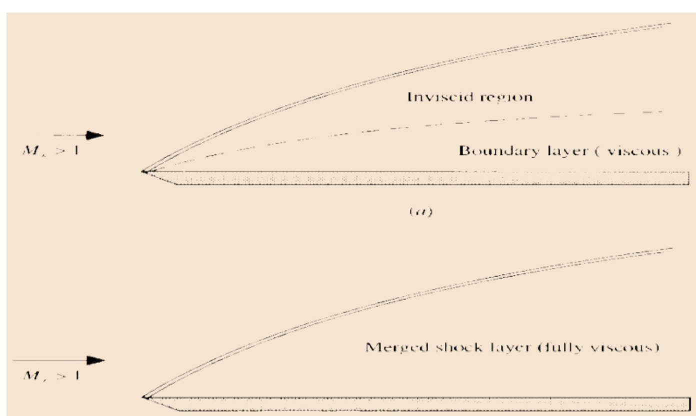

Fig 2. (a) Supersonic flow over a flat plate with a distinct boundary layer and region of inviscid flow. (b) Supersonic flow over a flat plate with a merged shock layer.

2.2 The Governing Flow Equations

2.2.1 Dimensional form

This problem is considered with interesting fluid phenomena. The advantage of using time-dependent Navier-Stokes approach is its inherent ability to evolve to the correct steady-state solution. Supersonic flow over a flat plate is modeled by a two dimensional unsteady compressible Navier-Stokes equations. The flow filed characteristics are obtained using the conservation of mass, momentum and energy equations. Two dimensional unsteady compressible Navier-Stokes equations by neglecting the body forces and volumetric heating are given below

Continuity equation

$$\frac{\partial p}{\partial t} + \frac{\partial(\rho u)}{\partial x} + \frac{\partial(\rho v)}{\partial y} = 0$$

X momentum equation

$$\frac{\partial(\rho u)}{\partial t} + \frac{\partial(\rho u^2 + p - \tau_{xx})}{\partial x} + \frac{\partial(\rho uv - \tau_{yx})}{\partial y} = 0$$

y momentum equation

$$\frac{\partial(\rho v)}{\partial t} + \frac{\partial(\rho uv - \tau_{xy})}{\partial x} + \frac{\partial(\rho v^2 + p - \tau_{yy})}{\partial y} = 0$$

Energy equation

$$\frac{\partial(\mathrm{E}_t)}{\partial t} + \frac{\partial((\mathrm{E}_t + p)u + q_x - u\tau_{xx} - v\tau_{xy})}{\partial x} + \frac{\partial((\mathrm{E}_t + p)v + q_x - u\tau_{yx} - v\tau_{yy})}{\partial y} = 0$$

Where t, x and y are the time x and y coordinates. ρ, u, v, p are the density, velocity in x direction and velocity in y direction and pressure respectively. E_t is the sum of kinetic energy and internal energy and $E_t = \rho\left(e + \frac{V^2}{2}\right)$. τ_{xx}, τ_{xy}, τ_{xx} are the shear stresses where

$$\tau_{xy} = \mu\left(\frac{\partial u}{\partial y} + \frac{\partial v}{\partial x}\right)$$

$$\tau_{xx} = \lambda\left(\frac{\partial u}{\partial x} + \frac{\partial v}{\partial y}\right) + 2\mu\frac{\partial u}{\partial x}$$

$$\tau_{yy} = \lambda\left(\frac{\partial u}{\partial x} + \frac{\partial v}{\partial y}\right) + 2\mu\frac{\partial v}{\partial y}$$

$$q_x = -k\frac{\partial T}{\partial x}$$

$$q_y = -k\frac{\partial T}{\partial y}$$

Where μ is dynamic viscosity.

This forms a system of four basic equations with nine unknown variables. For solving these equations, five additional equations used are the equation of state for a perfect gas, calorific equation of state, Sutherland's law for a calorifically perfect gas, resultant velocity equation and the relationship between Prandtl number and viscosity has been used. Free stream conditions are imposed on the front end of the flat plate. No slip situation is enforced on the flat plate and its temperature is assumed to be constant

$$p = \rho R T$$

$$e = c_v T$$

$$\mu = \mu_0 \left(\frac{T}{T_0} \right)^{3/2} \left(\frac{T_0 + 110}{T + 110} \right)$$

$$\Pr = 0.71 = \frac{\mu c_p}{k}$$

Where c_p is the specific heat at constant pressure (like c_v, a constant as long as the air is assumed calorically perfect). The system of equations is now closed: nine equations with nine unknowns.

The above equation can be write as

$$\frac{\partial U}{\partial t} + \frac{\partial E}{\partial x} + \frac{\partial F}{\partial y} = 0$$

Where U, E, and F are column vectors given by

$$U = \begin{Bmatrix} \rho \\ \rho u \\ \rho u^{2} \\ E_t \end{Bmatrix}$$

$$E = \begin{Bmatrix} \rho u \\ \rho u^{2} + p - \tau_{xx} \\ \rho u v - \tau_{xy} \\ (\mathrm{E}_t + p)u + q_x - u\tau_{xx} - v\tau_{xy} \end{Bmatrix}$$

$$F = \begin{Bmatrix} \rho v \\ \rho u v - \tau_{xy} \\ \rho v^{2} + p - \tau_{yy} \\ (\mathrm{E}_t + p)v + q_y - u\tau_{xy} - v\tau_{yy} \end{Bmatrix}$$

2.2.2 Non Dimensionalisation Governing Equation

The dimensionless governing equations are obtained using the following scales.

$$u^{*} = \frac{u}{u_{\infty}}, v^{*} = \frac{v}{u_{\infty}}, x^{*} = \frac{x}{x_{\infty}}, \mathrm{y}^{*} = \frac{y}{x_{\infty}}, p^{*} = \frac{p}{p_{\infty}}, \mathrm{t}^{*} = \frac{t u_{\infty}}{x_{\infty}}, \mu^{*} = \frac{\mu}{\mu_{\infty}}$$

and $\mathrm{q}_x = u_{\infty}^{3} \rho_{\infty} q_x^{*}$, $\qquad \mathrm{q}_y = u_{\infty}^{3} \rho_{\infty} q_y^{*}$

where

$$q_x^{*} = -\frac{\mu^{*}}{M_{\infty}^{2}(\gamma - 1)\mathrm{RePr}} \frac{dT^{*}}{dx^{*}}$$

$$q_y^{*} = -\frac{\mu^{*}}{M_{\infty}^{2}(\gamma - 1)\mathrm{RePr}} \frac{dT^{*}}{dy^{*}}$$

Continuity

$$\frac{\partial p^*}{\partial t^*} + \frac{\partial(\rho^* u^*)}{\partial x^*} + \frac{\partial(\rho^* v^*)}{\partial y^*} = 0$$

X momentum equation

$$\frac{\partial(\rho^* u^*)}{\partial t^*} + \frac{\partial\left(\rho^* u^{*2} + \frac{p^*}{(\gamma M^2)} - \frac{\tau^*{}_{xx}}{\mathrm{Re}}\right)}{\partial x^*} + \frac{\partial\left(\rho^* u^* v^* - \frac{\tau^*{}_{yx}}{\mathrm{Re}}\right)}{\partial y^*} = 0$$

y momentum equation

$$\frac{\partial(\rho^* v^*)}{\partial t^*} + \frac{\partial\left(\rho^* u^* v^* - \frac{\tau^*{}_{xy}}{\mathrm{Re}}\right)}{\partial x^*} + \frac{\partial\left(\rho^* v^{*2} + \frac{p^*}{(\gamma M^2)} - \frac{\tau^*{}_{yy}}{\mathrm{Re}}\right)}{\partial y^*} = 0$$

Energy equation

$$\frac{\partial(\rho^* e_t^*)}{\partial t^*} + \frac{\partial\left(\rho^* e_t^* u^* + \frac{p^*}{\Upsilon M^2} u^* - u^* \frac{\tau^*{}_{xx}}{\mathrm{Re}} - v^* \frac{\tau^*{}_{xy}}{\mathrm{Re}} + q^*{}_x\right)}{\partial x^*} + \frac{\partial\left(\rho^* e_t^* v^* + \frac{p^*}{\Upsilon M^2} v^* - u^* \frac{\tau^*{}_{xy}}{\mathrm{Re}} - v^* \frac{\tau^*{}_{yy}}{\mathrm{Re}} + q^*{}_y\right)}{\partial y^*} = 0$$

The compressible N-S equations in Cartesian coordinates without body forces or external heat addition can be written as

$$\frac{\partial U}{\partial t} + \frac{\partial E}{\partial x} + \frac{\partial F}{\partial y} = 0$$

Where U, E and F vector are given a

$$U=\begin{Bmatrix} \rho^{*} \\ \rho^{*} u^{*} \\ \rho^{*} v^{*} \\ \rho^{*} et^{*} \end{Bmatrix}$$

$$E=\begin{Bmatrix} \rho^{*} u^{*} \\ \rho^{*} u^{*2} + \dfrac{p^{*}}{\Upsilon M^{2}} - \dfrac{\tau^{*}_{xx}}{Re} \\ \rho^{*} u^{*} v^{*} - \dfrac{\tau^{*}_{xy}}{Re} \\ \rho^{*} et^{*} u^{*} + \dfrac{p^{*}}{\Upsilon M^{2}} u^{*} - u^{*} \dfrac{\tau^{*}_{xx}}{Re} - v^{*} \dfrac{\tau^{*}_{xy}}{Re} + q^{*}_{x} \end{Bmatrix}$$

$$F=\begin{Bmatrix} \rho^{*} v^{*} \\ \rho^{*} u^{*} v^{*} - \dfrac{\tau^{*}_{xy}}{Re} \\ \rho^{*} v^{*2} - \dfrac{\tau^{*}_{yy}}{Re} + \dfrac{p^{*}}{\Upsilon M^{2}} \\ \rho^{*} et^{*} v^{*} + \dfrac{p^{*}}{\Upsilon M^{2}} v^{*} - u^{*} \dfrac{\tau^{*}_{xy}}{Re} - v^{*} \dfrac{\tau^{*}_{yy}}{Re} + q^{*}_{y} \end{Bmatrix}$$

2.3 Initial and Boundary Conditions:

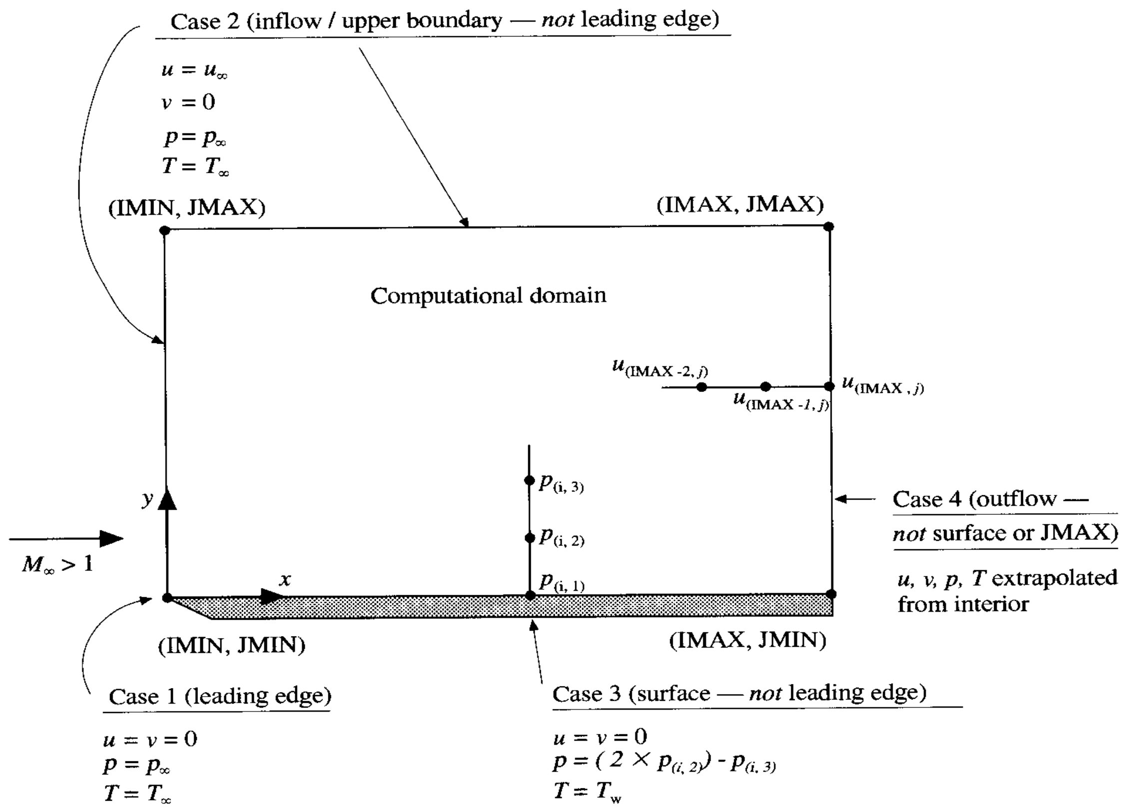

The value which has been considered for analysis:

Mach number = 4.0; Plate length (LHORI) = 0.00001 m; Sea level values for the freestream speed of sound, pressure, and temperature, respectively = 340.28 m/s, 101325.0 N/m 2, 288.16 K

The ratio of wall temperature to free stream temperature (T_w/T_∞ was set equal to 1.0; this ratio is convenient for investigating the impact of changing wall- temperature boundary conditions.

The ratio of specific heats (γ) = 1.4; The Prandtl number (Pr) = 0.71

Reference values (sea level) for dynamic viscosity and temperature, respectively = 1.7894 x 10 - 5 kg/(m. s), 288.16 K) ; Specific gas constant (R) = 287 J/(kg . K)

Chapter 3

The Numerical Method:

3.1. MacCormack's technique

MacCormack's technique is a variant of the Lax-Wendroff approach but is much simpler in its application. MacCormack method is an explicit finite-difference technique which is second-order-accurate in both space and time. First introduced in 1969, it became the most popular explicit finite-difference method for solving fluid flows for the next 15 years. Today, the MacCormack method has been mostly supplanted by more sophisticated approaches. However, the MacCormack method is very "student friendly;" it is among the easiest to understand and program. Moreover, the results obtained by using MacCormack's method are perfectly satisfactory for many fluid flow applications. For these reasons, MacCormack's method is highlighted here and will be used for some of the applications.

We can write the above equation as

$$\frac{\partial U}{\partial t} = -\frac{\partial E}{\partial x} - \frac{\partial F}{\partial y}$$

By MacCormack's time marching scheme (using Taylor's series)

$$U_{i,j}^{t+\Delta t} = U_{i,j}^{t} + \left(\frac{\partial U}{\partial t}\right)_{avg} \Delta t$$

Where

$$\left(\frac{\partial U}{\partial t}\right)_{avg} = \frac{1}{2}\left[\left(\frac{\partial U}{\partial t}\right)_{i,j}^{t} + \left(\overline{\frac{\partial U}{\partial t}}\right)_{i,j}^{t+\Delta t}\right]\Delta t$$

1. $(\partial U/\partial t)_{i,j}^{t}$ is calculated using forward spatial differences on the right-hand side of the governing equations from the known flow field at time t.

2. From step 1, PREDICTED values of the flow-field variables (denoted by a bar) can be obtained at time t + Δt, as follows:

$$\overline{U}_{i,j}^{t+\Delta t} = U_{i,j}^{t} + \left(\frac{\partial U}{\partial t}\right)_{avg} \Delta t$$

Combining steps 1 and 2, predicted values are determined as follows:

$$\overline{U}_{i,j}^{t+\Delta t} = U_{i,j}^{t} - \frac{\Delta t}{\Delta x}\left(E_{i+1}^{t} - E_{i}^{t}\right) - \frac{\Delta t}{\Delta y}\left(F_{j+1}^{t} - F_{j}^{t}\right)$$

3. Using rearward spatial differences, the predicted values (from step 2) are inserted into the governing equations such that a predicted time derivative $\left(\partial\overline{U}/\partial t\right)_{i,j}^{t}$ can be obtained.

4. Finally, substitute $\left(\partial U/\partial t\right)_{i,j}^{t}$ (from step 3) into Eq. to obtain CORRECTED second-order-accurate values of U at time t + Δt .By steps 3 and 4 are combined as follows:

$$U_{i,j}^{t+\Delta t} = \tfrac{1}{2}\left[U_{i,j}^{t} + \overline{U}_{i,j}^{t+\Delta t} - \frac{\Delta t}{\Delta x}\left(\overline{E}_{i+1}^{t} - \overline{E}_{i}^{t}\right) - \frac{\Delta t}{\Delta y}\left(\overline{F}_{j+1}^{t} - \overline{F}_{j}^{t}\right)\right]$$

Steps 1 to 4 are repeated until the flow-field variables approach a steady-state value; this is the desired steady-state solution.

To maintain second-order accuracy, the x-derivative terms appearing in E are differenced in the opposite direction to that used for ∂E/∂x, while the y-derivative terms are approximated with central differences. Likewise, the y-derivative terms appearing in F are differenced in the opposite direction to that used for ∂F/∂y, while the x-derivative terms in F are approximated with central differences.

After each predictor or corrector step, the primitive variables are obtained by decoding the U vector, as shown below;

$$\rho = U_1$$

$$u = \frac{\rho u}{\rho} = \frac{U_2}{U_1}$$

$$v = \frac{\rho v}{\rho} = \frac{U_3}{U_1}$$

$$E_t = \rho\left(e + \frac{V^2}{2}\right) = U_4$$

$$\text{or } e = \frac{U_4}{U_1} - \frac{u^2 + v^2}{2}$$

With p, u, v, and e determined, the remaining flow-field properties can be obtained by using the equations as follows:

$$T = \frac{e}{c_v}$$

$$p = \rho RT$$

μ and k are functions of temperature T. μ can be determined by applying Sutherland's law. Once μ is known, a constant Prandtl number assumption leads directly to k, as shown below

$$k = \frac{\mu c_p}{\Pr}$$

Because of the complexity of the compressible N-S equations, it is not possible to obtain a closed-form stability expression for the MacCormack scheme applied to these equations. However, the following empirical formula can normally be used:

$$\Delta t \le \frac{\sigma\left(\Delta t\right)_{CFL}}{1 + 2/\text{Re}_{\Delta}}$$

Where σ is the safety factor ($\cong 0.9$), $\left(\Delta t\right)_{CFL}$ is the inviscid Courant-Friednchs- Levy (CFL) condition

$$(\Delta t)_{CFL} \le \left(\frac{|u|}{\Delta x} + \frac{|v|}{\Delta y} + a\sqrt{\left(\frac{1}{(\Delta x)^2} + \frac{1}{(\Delta y)^2} \right)} + 2v'_{i,j}\left(\frac{1}{(\Delta x)^2} + \frac{1}{(\Delta y)^2} \right) \right)^{-1}$$

where

$$v'_{i,j} = \max\left[\frac{\frac{4}{3}\mu_{i,j}\left(\gamma\,\mu_{i,j} / \mathrm{Pr}\right)}{\rho_{i,j}} \right]$$

Re_{Δ} is the minimum mesh Reynolds number given by

$$\mathrm{Re}_{\Delta} = \min\left(\mathrm{Re}_{\Delta x}, \mathrm{Re}_{\Delta y}\right)$$

Where

$$\mathrm{Re}_{\Delta x} = \frac{\rho |u| \Delta x}{\mu}$$

$$\mathrm{Re}_{\Delta y} = \frac{\rho |v| \Delta y}{\mu}$$

and a is the local speed of sound,

$$a = \sqrt{\frac{\gamma p}{\rho}}$$

Before each step, Δt can be computed for each grid point using above equation). The smallest value of Δt is then used to advance the solution over the entire mesh. If only the steady-state solution is desired, Li (1973) has suggested that the solution at each point be advanced using the maximum possible Δt, as computed from above equation, in order to accelerate the convergence of the solution. This procedure is referred to as local time stepping. In addition, multigrid procedures can also be used to accelerate the convergence of N-S calculations.

3.2 Artificial Viscosity addition to MacCormack by Jameson's method:-

The Navier Stokes equations require some artificial viscosity in order have stability and smoothing of the solution. Adding viscosity also helps in rapid convergence towards the solution. Here artificial viscosity is added in the predictor and corrector step as follows,

1. Predictor step:-

$$\overline{U}_{i,j}^{t+\Delta t} = U_{i,j}^{t} + \left(\frac{\partial U}{\partial t}\right)_{i,j} \Delta t + S_{i,j}^{t}$$

Where $S_{i,j}^{t}$ artificial viscosity which is given by,

$$S_{i,j}^{t} = c_x \gamma_1 \left(U_{i+1,j}^{t} - 2U_{i,j}^{t} + U_{i-1,j}^{t}\right) + c_y \gamma_2 \left(U_{i,j+1}^{t} - 2U_{i,j}^{t} + U_{i,j-1}^{t}\right)$$

where

$$\gamma_1 = \frac{\left|p_{i+1,j}^{t} - 2p_{i,j}^{t} + p_{i-1,j}^{t}\right|}{\left|p_{i+1,j}^{t}\right| + 2\left|p_{i,j}^{t}\right| + \left|p_{i-1,j}^{t}\right|} \quad , \quad \gamma_2 = \frac{\left|p_{i,j+1}^{t} - 2p_{i,j}^{t} + p_{i,j-1}^{t}\right|}{\left|p_{i,j+1}^{t}\right| + 2\left|p_{i,j}^{t}\right| + \left|p_{i,j-1}^{t}\right|}$$

2. Corrector step:-

$$U_{i,j}^{t+\Delta t} = U_{i,j}^{t} + \left(\frac{\partial U}{\partial t}\right)_{avg} \Delta t + \overline{S}_{i,j}^{t}$$

Where $\overline{S}_{i,j}^{t}$ artificial viscosity which is given by,

$$\overline{S}_{i,j}^{t} = c_x \gamma_3 \left(\overline{U}_{i+1,j}^{t} - 2\overline{U}_{i,j}^{t} + \overline{U}_{i-1,j}^{t} \right) + c_y \gamma_4 \left(\overline{U}_{i,j+1}^{t} - 2\overline{U}_{i,j}^{t} + \overline{U}_{i,j-1}^{t} \right)$$

where

$$\gamma_3 = \frac{\left| \overline{p}_{i+1,j}^{t} - 2\overline{p}_{i,j}^{t} + \overline{p}_{i-1,j}^{t} \right|}{\left| \overline{p}_{i+1,j}^{t} \right| + 2\left| \overline{p}_{i,j}^{t} \right| + \left| \overline{p}_{i-1,j}^{t} \right|} \quad , \quad \gamma_4 = \frac{\left| \overline{p}_{i,j+1}^{t} - 2\overline{p}_{i,j}^{t} + \overline{p}_{i,j-1}^{t} \right|}{\left| \overline{p}_{i,j+1}^{t} \right| + 2\left| \overline{p}_{i,j}^{t} \right| + \left| \overline{p}_{i,j-1}^{t} \right|}$$

Pressure and conservative variables used to calculate artificial viscosity in corrector step are predicted values of pressure and conservative variables. Since the artificial dissipation term is of third order, the overall accuracy of the scheme is of second order.

3.3. Runge Kutta Method

Runge –Kutta fourth order (RK4) method is fourth order accuracy with time. This method is more stable than other time integration schemes.

Runge Kutta method is a powerful tool for the solution of differential equations. Most of the research has been oriented towards improving the accuracy or the flexibility problems of the classical Runge Kutta method’. A particular problem of this type describing the supersonic flow over a flat plate a is investigated. The equation representing this phenomenon is non-linear in nature.

For the higher order of accuracy and fast convergence of solution we can use the Runge Kutta method. This method give us fourth order of accuracy while MacCormack scheme give us second order of accuracy. Sometime MacCormack scheme is not stable for particular value problem or very sensitive. So we can try that Runge Kutta method.

Our system of equation is of type

$$\frac{\partial U^{t}_{i,j}}{\partial t} = f(\mathrm{x}, \mathrm{y}, \mathrm{t})$$

$$U^{t+\Delta t}_{i,j} = U^{t}_{i,j} + \frac{1}{6}\left(k_1 + 2\left(k_2 + k_3\right) + k_4\right)$$

Where

$$k_1 = f(\mathrm{g}(x_{i,j}, \mathrm{y}_{i,j}), t)$$
$$k_2 = f(\mathrm{g}(x_{i,j}, \mathrm{y}_{i,j}) + \frac{k_1}{2}, t + \frac{\Delta t}{2})$$
$$k_3 = f(\mathrm{g}(x_{i,j}, \mathrm{y}_{i,j}) + \frac{k_2}{2}, t + \frac{\Delta t}{2})$$
$$k_2 = f(\mathrm{g}(x_{i,j}, \mathrm{y}_{i,j}) + k_3, t + \Delta t)$$

Algorithm:

1. First we find k_1 for all set of equation simultaneously by forward difference method by using initial and boundary value and update the free stream variables
2. Similarly we find k_2, k_3, k_4 and by backward –forward difference method and update the variables after each step.
3. Find the U set variable by using above equation at new time step and update the value till state solution.

Chapter 4.

Results and Discussions:

4.1. Validation:

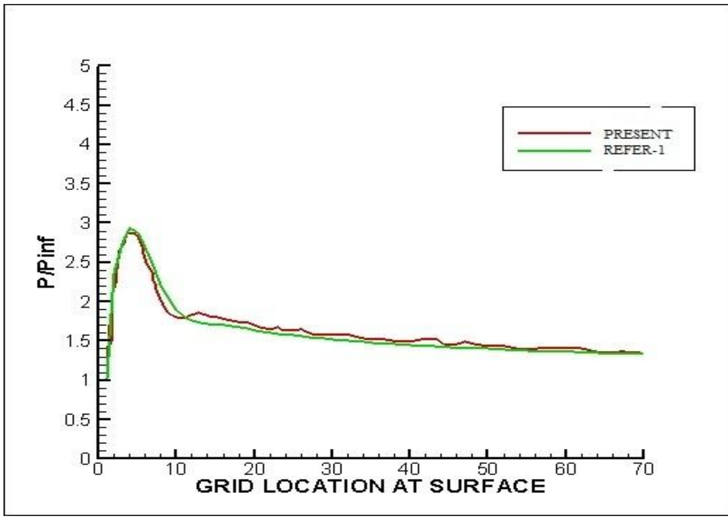

fig 4.1 pressure along the surface at leading edge

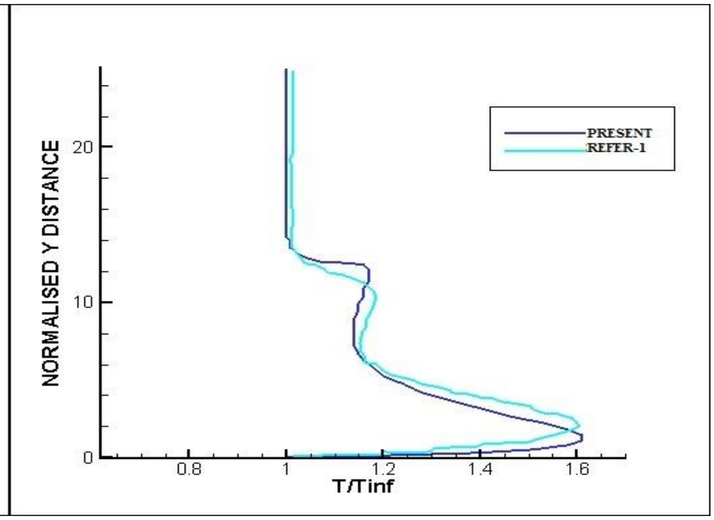

fig 4.2 temperature plot at trailing edge Fig

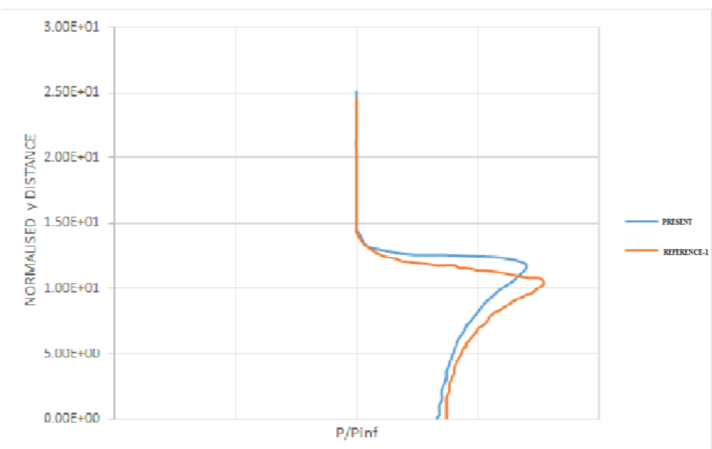

fig 4.3 pressure vs normalized Y distance at trailing edge

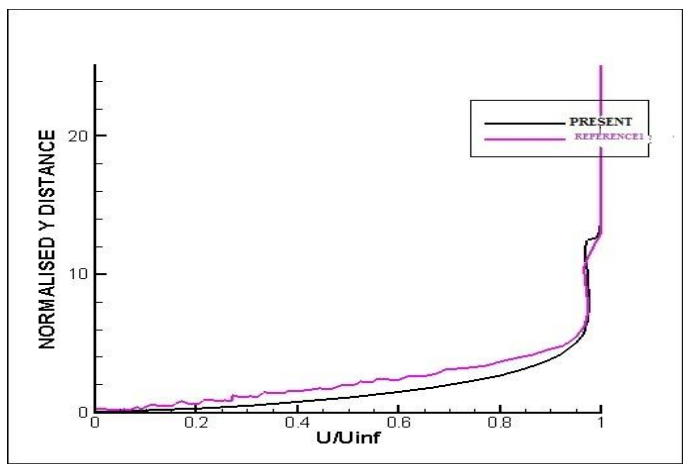

fig 4.4 u-velocity profile at trailing edge

4.2. Reference Results:

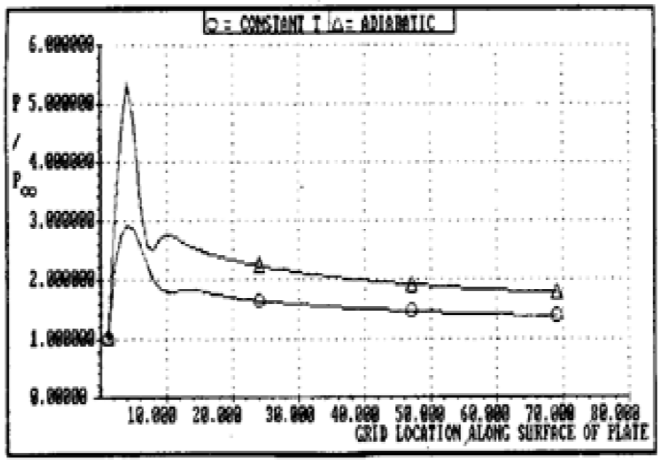

Fig 4.5

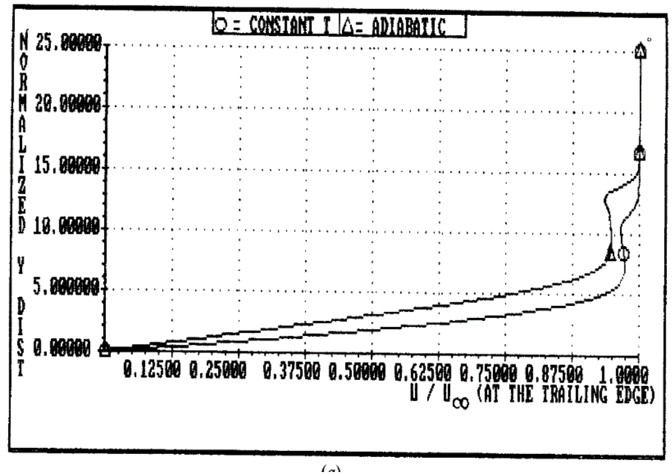

fig 4.6

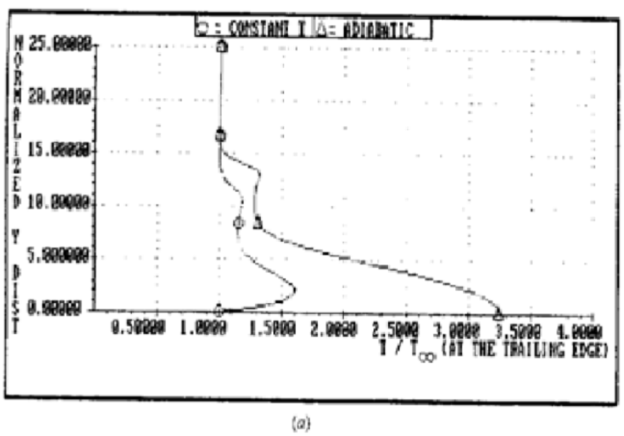

Fig 4.7

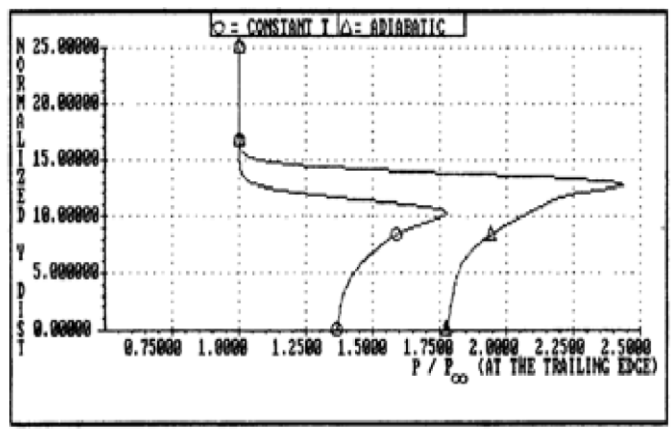

fig 4.8

Here for validation of result is shown for constant wall temperature. Pressure plot along the surface (fig 4.1), temperature plot (fig 4.2), u –velocity plot(fig 4.4), pressure plot(fig 4.4) at trailing edge are plotted here and try to compare the reference results. This is almost same by appearance.

4.3 Plots for different Mach numbers:

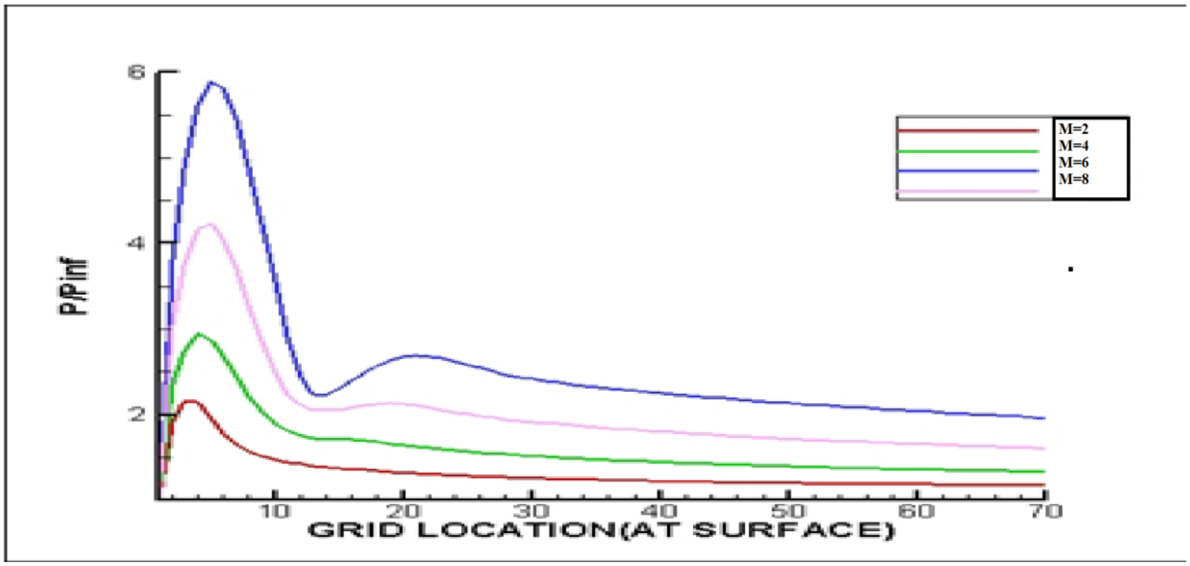

Fig: 4. 9

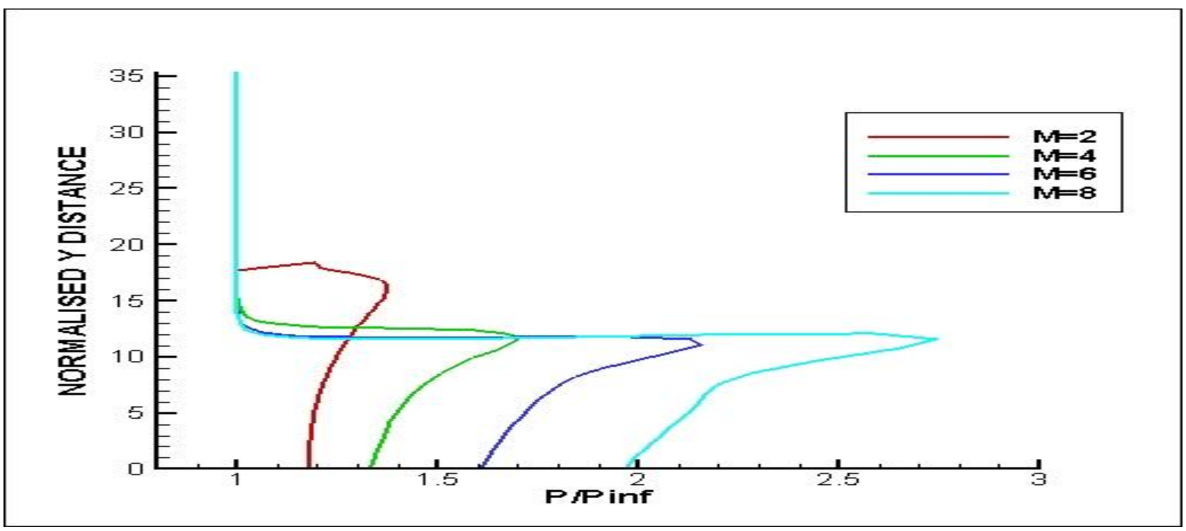

Fig: 4. 10

From fig 4.9and fig: 4. 10 the pressure distribution in the entire flow field has been computed. The normalised pressure distribution at the leading edge and trailing edge for the inflow velocity with different Mach numbers is plotted. It has been observed that due to the formation of boundary layer, the flow velocity decreases and hence pressure increases as shown by the plot for different Mach numbers at the trailing edge. With the increase in the Mach numbers, the non-dimensional pressure is also increasing at the trailing edge

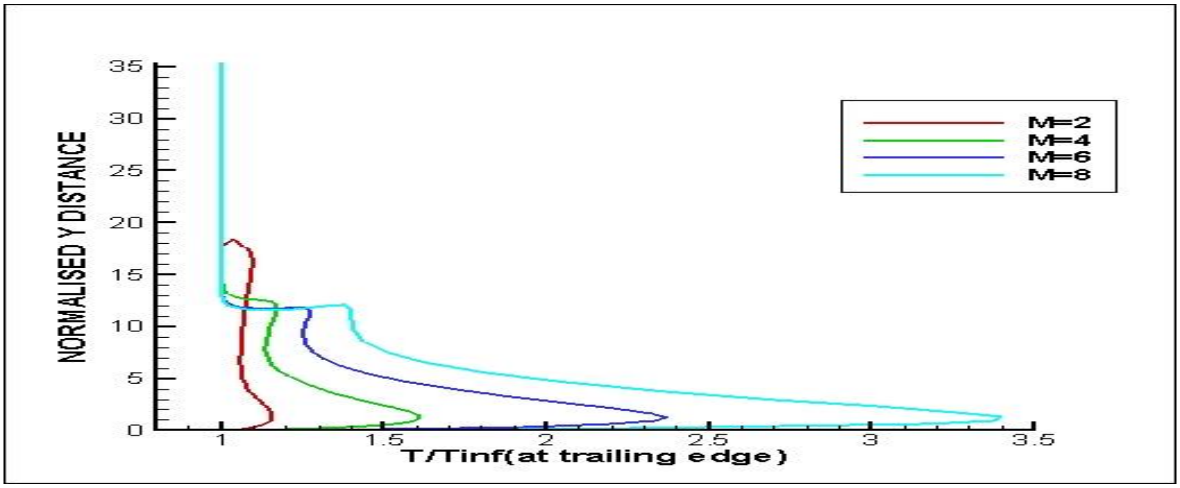

Fig: 4. 11

From fig 4.11 the temperature distribution in the entire flow field has been computed. The normalised temperature distribution at the trailing edge for the inflow velocity with different i-location is plotted. It has been observed that due to the formation of boundary layer, the temperature increases as shown by the plot for different i-location in the trailing edge. With the increase in the Mach numbers, the non-dimensional temperature is also increasing at the trailing edge.

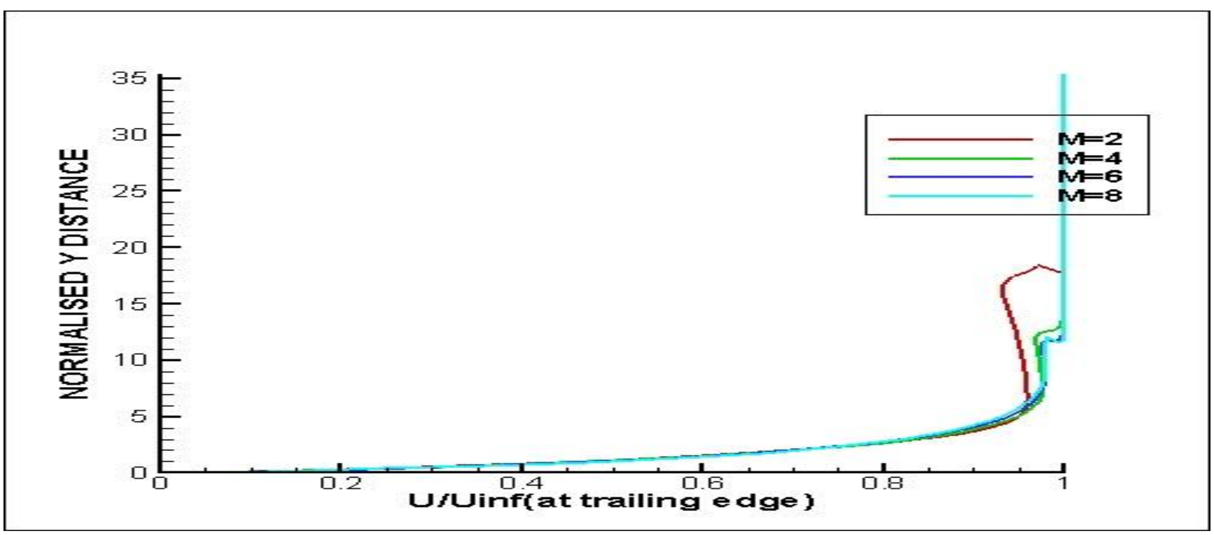

Fig: 4. 12

From fig 4.12 the velocity distribution in the entire flow field has been computed. At the plate surface the velocity is zero because of no-slip condition. Towards the vertical direction the velocity gradually increases to the free stream condition

4.4 Plots for different Wall Temperatures:

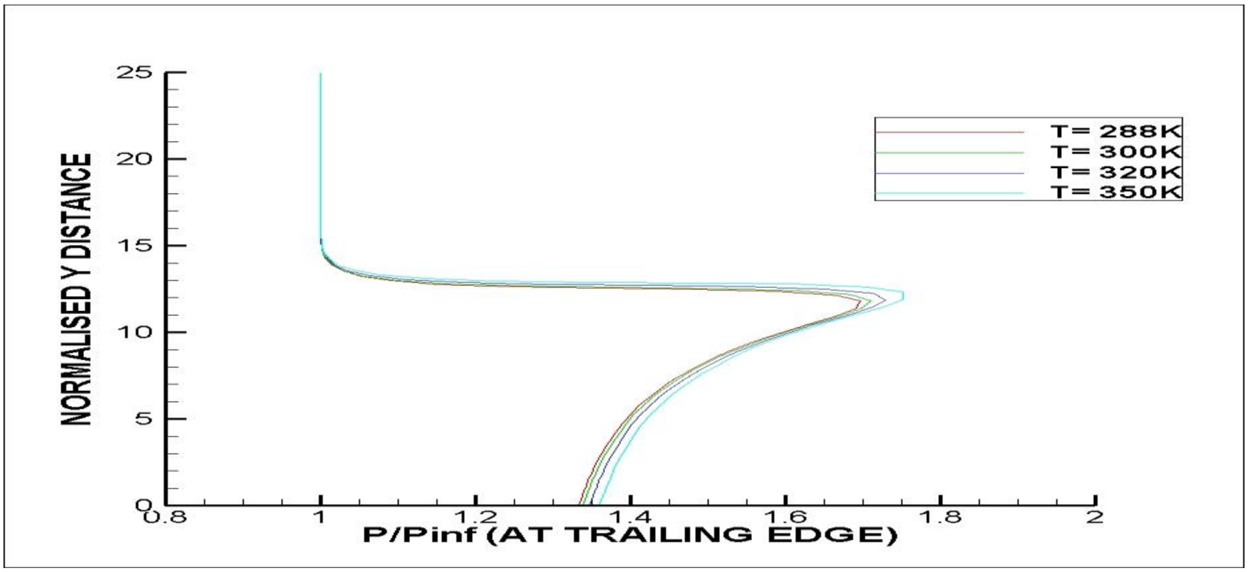

FIG 4.13

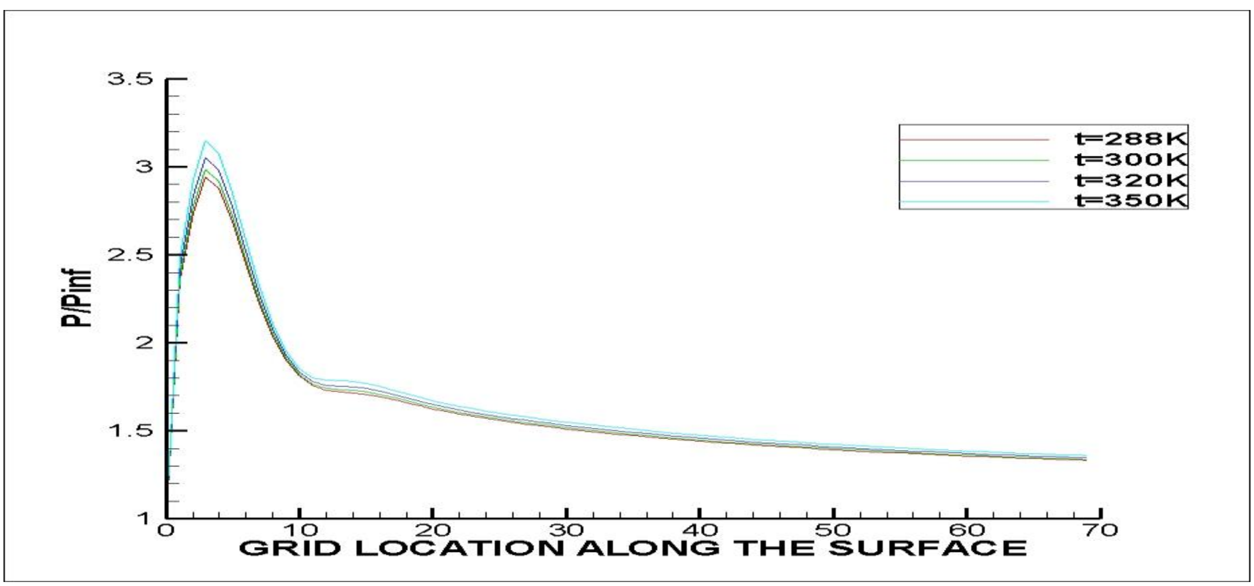

FIG 4.14

From fig 4.13 and fig 4.14 this is a non-dimensional pressure profile at the leading edge and trailing edge. At the adiabatic conditions it seems that the overall pressure increases above the constant temperature condition. The result is a relatively lower density and hence thicker boundary layer therefore it create a strong leading edge shockwave thus increase the pressure within the shock layer.

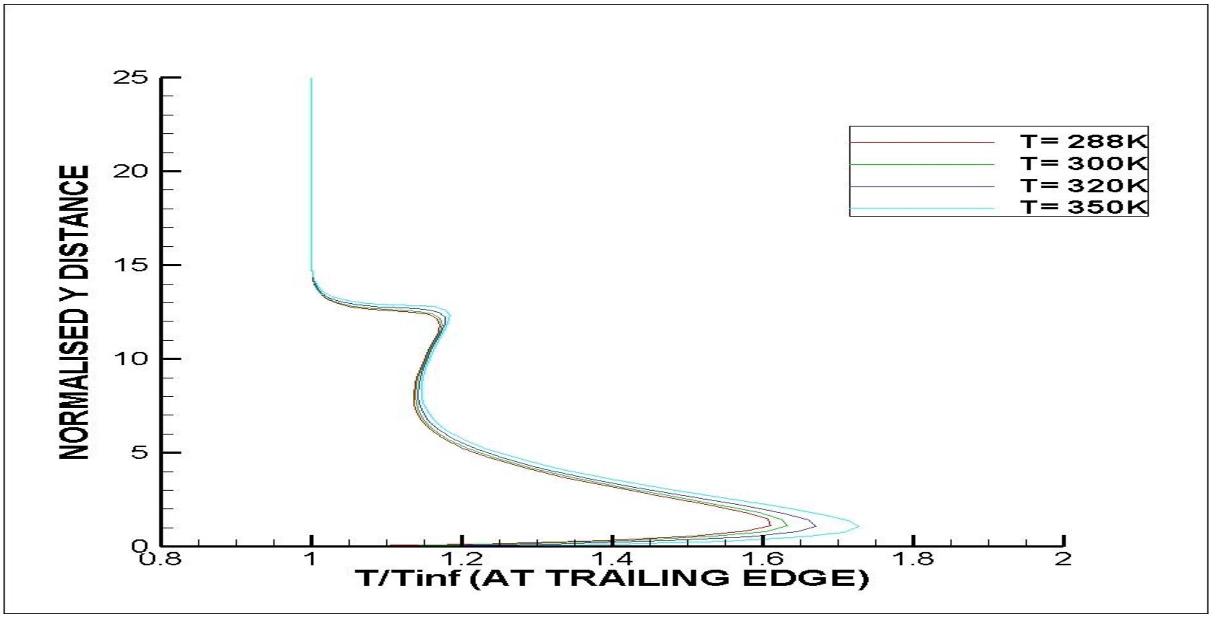

Fig 4.15

Similarly in Fig 4.15 at the adiabatic conditions it seems that the overall temperature increases above the constant temperature condition. The result is a relatively lower density and hence thicker boundary layer therefore it create a strong leading edge shockwave thus increase the pressure within the shock layer

4.4 Contour plots:

4.1 U-Velocity Contour

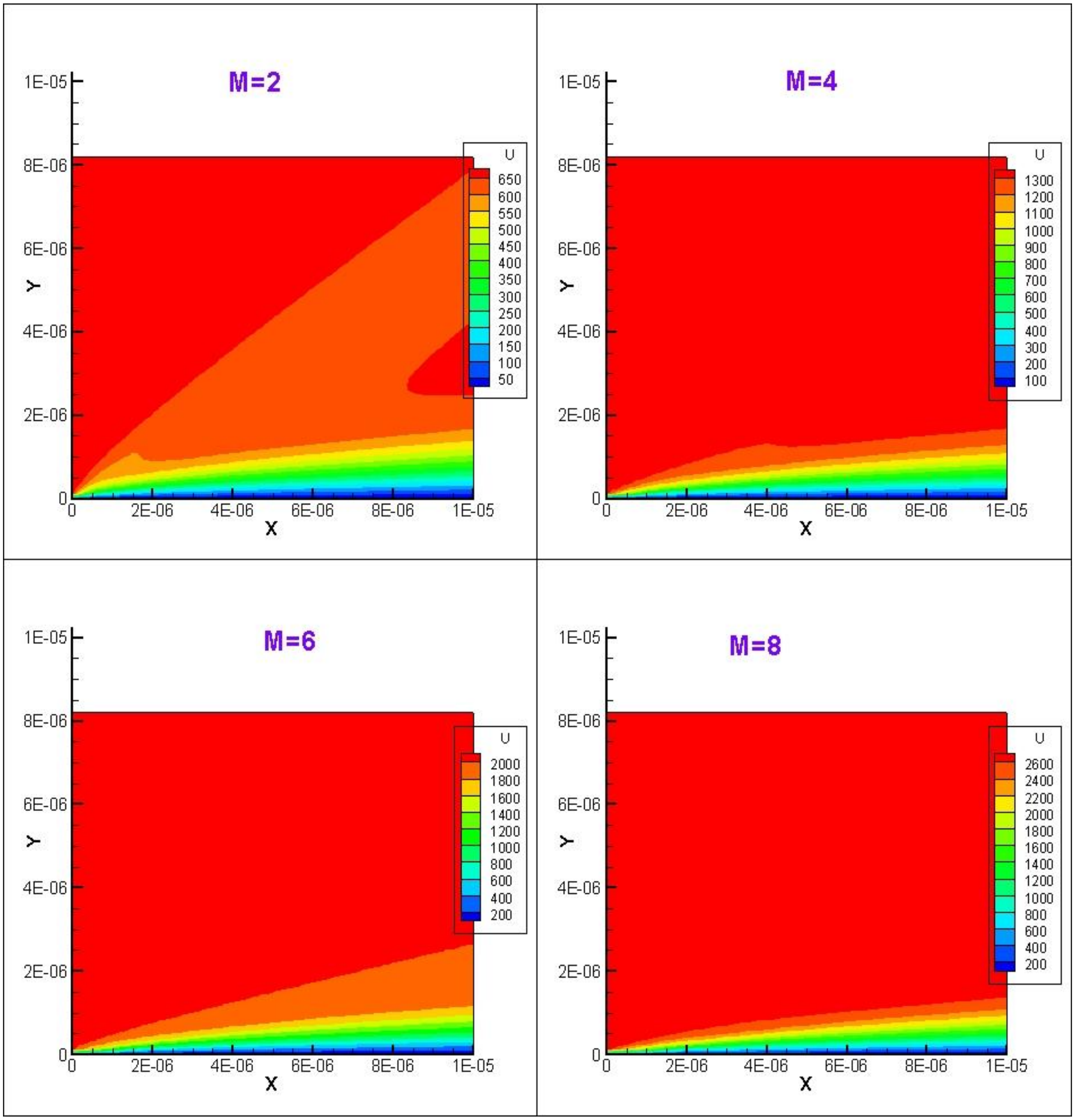

FIG 4.16

4.2 Temperature Contour

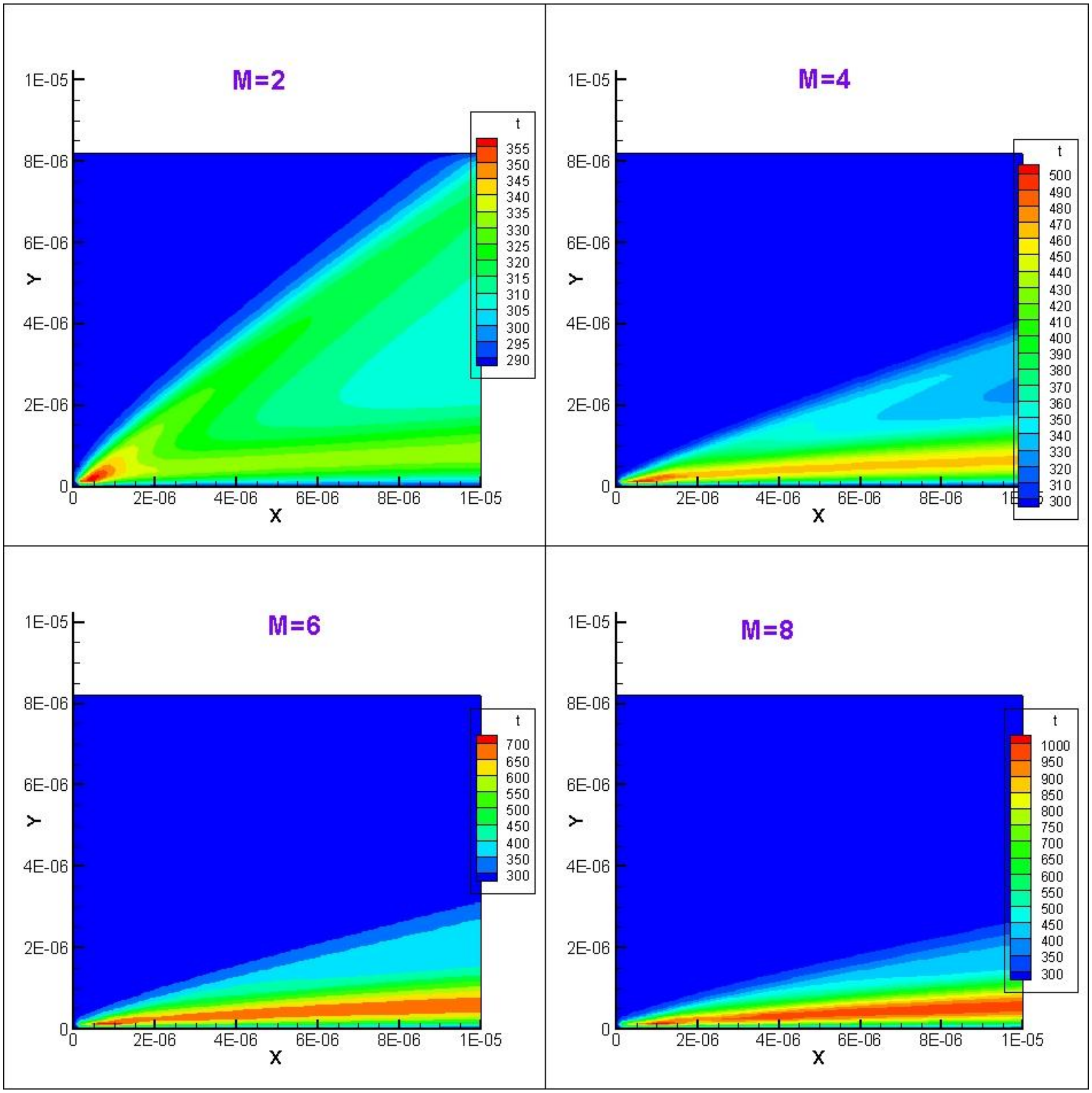

FIG 4.17

4.3 Pressure Contour

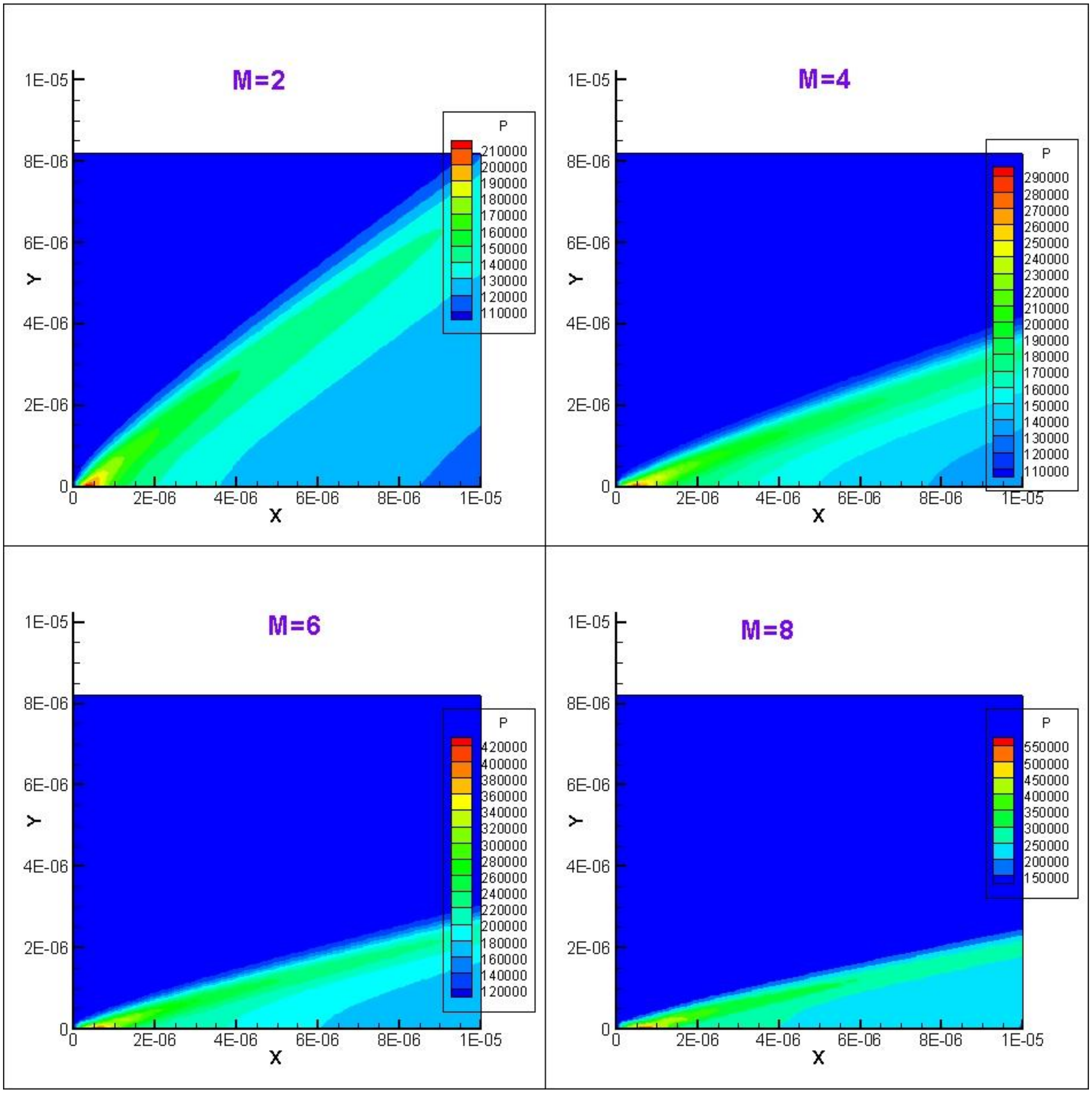

FIG 4.18

4.4 Density Contour

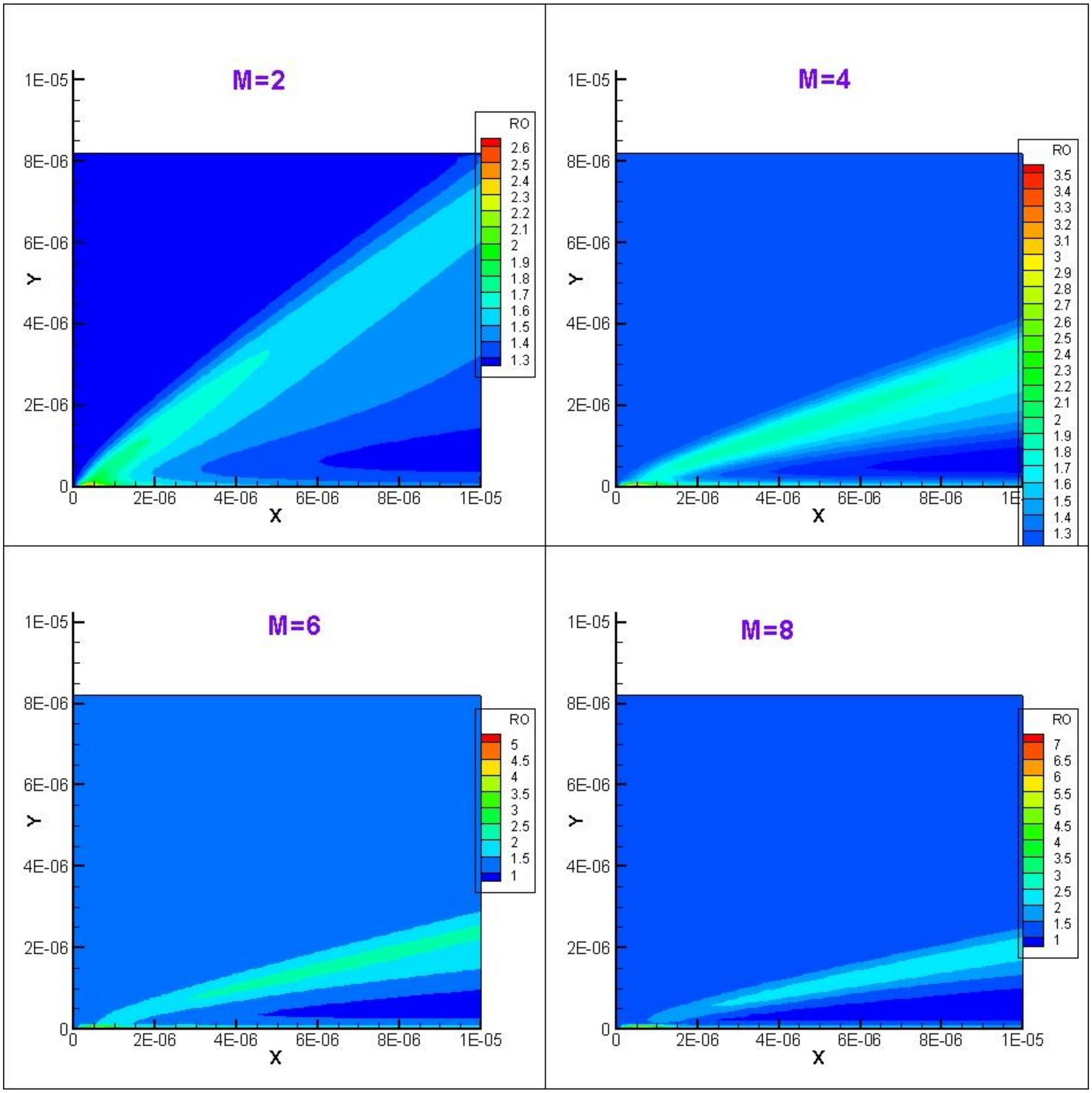

FIG 4.19

From the above contour (FIG 4.16, FIG 4.17, FIG 4.18, FIG 4.19) we observe that shocks wave move along the surface when we increase the Mach number. And shocks strength increase with increase the Mach number.

Chapter 5

Conclusions:

Supersonic flow over a flat plate has been investigated numerically and reported here. The effect of free stream Mach number and wall temperature on shock/boundary layer interactions are reported here. The following conclusions are obtained from the present investigation.

- Shock formation near the leading of the plate.
- Shock strength increases with increase in free stream Mach number.
- Shock moves near to the surface with increase in free stream Mach number.
- The velocity boundary layer thickness decreases with increase in free stream Mach number.
- Shock strength increases with increase in wall temperature.
- The velocity boundary layer thickness decreases with increase in wall temperature.
- Significant change of surface pressure with increase of free stream Mach number and wall temperature.

Chapter 6

References

[1] John D. Anderson, Jr.: Computational Fluid Dynamics, McGraw-Hill, Inc.

[2] John D. Anderson, Jr.: Fundamentals of Aerodynamics, McGraw-Hill, Inc.

[3] John D. Anderson, Jr.: Hypersonic and High Temperature Gas Dynamics, McGraw-Hill, Inc.

[4] R. W. MacCormack, "A Numerical Approach for solving equations of compressible viscous flow," AIAA J. 20, 1275 (1982).

[5] Schichting, H.: Boundary Layer Theory, McGraw-Hill, Inc.

[6] Patankar, S. V.: Numerical Heat Transfer and Fluid Flow, McGraw-Hill, Inc.

[7] Fletcher, C.A.: Computational Techniques for Fluid Dynamics, Springer-Verlag, Berlin,1988.

[8] T. J. Chung, Computational Fluid Dynamics, Cambridge.

[9].Jameson, A., Schmidt, W., and Turkel, E., "Numerical Solutions of the Euler Equations by Finite Volume Methods Using Runge-Kutta Time-Stepping Schemes," AIAA Paper 81-1259, 1981.

[10]. Rizzi, A. and Eriksson, L., "Explicit Multistage Finite Volume Procedure to Solve the Euler Equations for Transonic Flow," *Lecture Series on Computational Fluid Dynamics,* von Karman Institute, Rhode-St-Genese, Belgium, 1983

[11] Y. Morinishi, T. Lund, O. Vasilyev, P. Moin, Fully conservative higher order finite difference schemes for incompressible flows, J. Comput. Phys. 143(1998) 90–124.

[12] R. Knikker, Study of a staggered fourth-order compact scheme for unsteady incompressible viscous flow, Int. J. Numer. Methods Fluids 59 (2009) 1063–1092.

[13] N. Nikitin, Third-order-accurate semi-implicit Runge–Kutta scheme for incompressible Navier–Stokes equations, Int. J. Numer. Methods Fluids 51(2006) 221–233.

[14] J. Pereira, M. Kobayashi, J. Pereira, A fourth-order-accurate finite volume compact method for the incompressible Navier–Stokes equations, J. Comput.Phys. 167 (2001) 217–243.

[15] N. Kampanis, J. Ekaterinaris,

[16] Anderson, B.H., Jon Tinapple and Lewis Surber.,"Optimal Control of Shock Wave Turbulent Boundary Layer Interactions using Micro Array Actuation",3rd AIAA Flow Control Conference, 5 - 8 June 2006,San Francisco, California.

[17] Adam Huang., James Lew., Yong Xu., Yu- Chong Tai and Chih- Ming Ho., "Micro Sensors and Actuators for Macro Fluidic Control", IEEE Sensors Journal,

Vol.4. No.4 August, 2004, pp.494-501.

[18] Mehul, P. Patel., Javier Lopera and Terry T. Ng., "Active Boat Tailing and Aerodynamic Control Fins for Maneuvering Weapons", 2nd AIAA Flow Control Conference, 28 June to 01 July, 2004, Portland, OR.

[19]. Smith, F.T., "Laminar Flow Over a Small Hump on a Flat Plate", Journal of Fluid Mechanics, Vol. 57, No.4, March, 1973, pp.803-824.

[20]. Dolling D.S. and Murphy M.T., "Unsteadiness of the Separation Shock Wave Structure in a Super Sonic Compression Ramp Flow Field", AIAA Journal, Vol.21. No.12, December, 1983, pp.1628-1634.

[21]. Chapman, D. R., Kuehn, D. M. and Larson, H. K., "Investigation of Separated Flows in Supersonic and Subsonic Streams with Emphasis on the Effect of Transition", NACA TR 1356, 1957.

[22]. Efimtsov, B. M., Rizzi, S. A., Andersson, A. O. and Andrianov, E. V., "Influence of Small Steps on Wall Pressure Fluctuation Spectra Measured on TU- 144LL Flying Laboratory", AIAA Paper 2002-2605,June, 2002.

[23].Carter, J.E., "Numerical Solution of the Navier- Strokes Equation for the Supersonic Laminar Flow over Two Dimensional Compression Corner", NASA TR R-385, 1972.

[24]. Degani, D. and Stegger, J.L., "Comparison Between Navier-Stokes and Thin Layer Computations for Separated Supersonic Flow", AIAA Journal, Vol.21, No.11, 1983, pp.1604-1606.

[25]. Steger, J. L. and Warming, R. F., "Flux Vector Splitting of the Inviscid Gas Dynamic Equations with Applications to Finite Difference Methods," *Journal of Computational Physics,* Vol. 40, April 1981, pp. 263-293.

[26]. Roe, P. L., "The Use of the Riemann Problem in Finite Difference Schemes," *Seventh International Conference on Numerical Methods in Fluid Dynamics,* Stanford, CA, 1980.

[27]. Van Leer, B., "Flux-Vector Splitting for the Euler Equations," *Eighth International Conference on Numerical Methods in Fluid Dynamics, Springer Lecture Notes in Physics No. 170,* edited by E. Krause, 1983.

[28]. Osher, S. and Chakravarthy, S., "Upwind Schemes and Boundary Conditions with Applications to Euler Equations in General Geometries," *Journal of Computational Physics,* Vol. 50, 1983, pp.447-481.

[29]. Computational Study of Supersonic Flow Over a Flat Plate with Protrusion Deshpande V, Eshpuniyani B, Sanghi S Journal of Aerospace Science and Technologies 01/2011; 63(4):266-276.

[30]. Goldman R.L., Morkovin M.V., Schumacher R. N.,1968. Unsteady Control Surface Loads of Lifting Re-entry Vehicles at Very High Speeds, AIAA Journal 6(1) pp. 44-50.

[31]. Park S. O., Chung Y. M. and Sung H. J., 1994. Numerical Study of Unsteady Supersonic Compression Ramp Flows, AIAA Journal, 32(1) pp. 216-218.

[32].Park S. O., Lee C. H. and Kang K. M., 2003.Viscous Supersonic Flow Over Moving Compression Ramp, AIAA Journal, 41(1) pp. 133-137.

[33]. Ami Harten, Bjorn Engquist, Stanley Osher, and Sukumar R Chakravarthy. Uniformly high order accurate essentially non-oscillatory schemes, {III}. *Journal of Computational Physics*, 71(2):231 – 303, 1987.

[34] P. Spalart, R. Moser, M. Rogers, Spectral methods for the Navier–Stokes equations with one infinite and two periodic directions, J. Comput. Phys. 96(1991) 297–324.

[35] H. Le, P. Moin, An improvement of fractional step methods for the incompressible Navier–Stokes equations, J. Comput. Phys. 92 (1991) 369–379.